Characterization of Al Parts Fabricated by Additive Friction Stir (AFS) Manufacturing

Cecilia Stoner, Marcia Domack, Eric Hoffman

Advanced Materials and Processing Branch, NASA Langley Research Center, Hampton VA

CELEBRATING 100 YEARS — NASA Langley Research Center 1917-2017

Motivation

Within the rapidly expanding realm of additive manufacturing, the need for efficient printing of alloys with robust as-deposited microstructures is critical. While there has been much success in the selective laser melting (SLM) process of achieving printed parts with acceptable microstructures and a fine feature resolution, such powder-based methods can be tremendously slow when considering production scale processing. Furthermore, the layer-by-layer powder deposition in an inert environment places restrictions on the utility of SLM technology – such as in-space repair of structural components or on-component deposition – thus reducing the versatility of that particular process.

An emerging method of additive manufacturing is additive friction stir (AFS) processing, which involves the solid-state deposition of rod or powdered alloy or metal matrix composite (MMC) material through plastically deforming the filler material into a substrate and creating fully-dense parts at much higher speeds than achievable by other additive methods. The solid-state nature of AFS deposition results in a microstructure more similar to wrought material than to the cast-like microstructure of fusion-based processes like SLM, and causes more homogenous deposition of solute content and MMC reinforcement since there is no molten pool in which particles may segregate.

AFS Deposition Process

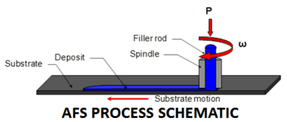

AFS PROCESS SCHEMATIC

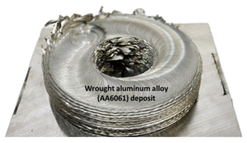

AFS AM DEMONSTRATION (6 in. OD)

Image from: NASA AFS SBIR Phase I

- Solid state process performed at room temperature without shielding gas
- Feedstock transported through rotating hollow spindle is deposited on a substrate to create a fully dense part
- Many materials viable for deposition: steel, aluminum, magnesium, MMC

Samples Characterized in this Experiment

- Aluminum alloys 2219 and 2139 were deposited in stringers of various heights for extraction of tensile and compact tension specimens, as well as metallography samples
- The 2219 and 2139 samples were divided into three groups for heat treatment: as-deposited, solution heat treated (SHT) and aged, and direct aged (no SHT)
- Techniques employed across these samples include microstructural characterization, mechanical properties testing (tensile, fracture toughness, hardness), and x-ray computed tomography (XCT) scanning for defects
- Four aluminum alloy 6061+SiC MMC deposits of varying vol% SiC, including a functionally graded structure, for SiC percent reinforcement analysis

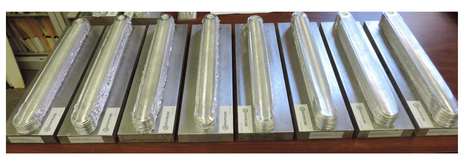

Aluminum 2219 and 2139 samples

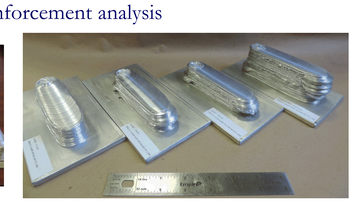

Aluminum 6061 + SiC samples

Objective

Conduct initial characterization of aluminum parts provided by a partner company and fabricated with AFS processing to observe the microstructural and mechanical properties of additively manufactured Al 2219, 2139, and 6061-SiC metal matrix composites (MMCs).

Macros of Samples Before/After Heat Treatment

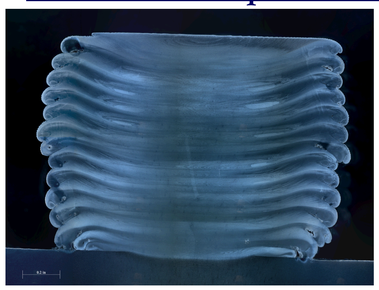

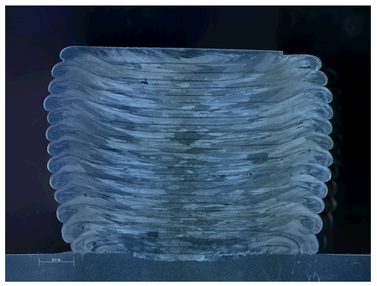

Above are images of the 2139 as-deposited sample (left) and the 2219 solution heat treated and aged sample (right), which display the fine and coarser grain microstructure of the samples, respectively, as well as visible deposit layers. The direct aged samples appeared most similar to the as-deposited structures. The outer, scalloped regions of the deposits are termed "flash" and are removed via post-machining.

Longitudinal (L) vs. Short Transverse (ST) Tensile Testing

Tensile testing was performed on specimens in the as-deposited and direct aged conditions for both the 2219 and 2139 alloys, since these heat treatment conditions exhibited less cracking than the solution heat treated and aged deposits. Tensile samples were oriented parallel to the build direction (L) as well as through the thickness of the build (ST) to examine strength along and across deposit layers.

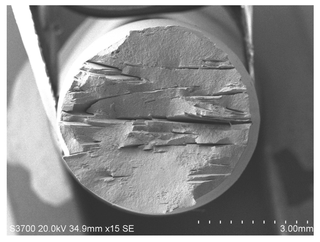

L tensile specimen

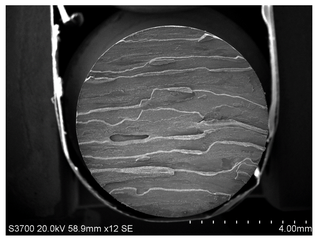

ST tensile specimen

Below are the data obtained from the tensile testing. It can be seen that the 2139 samples had a higher strength than the 2219 specimens, as is also the case in wrought product of the alloys. The L tensile samples also outperformed the ST tensile samples, likely due to insufficient bonding between layers that may have contributed to the previously noted cracking problem. It can be seen that the 2219 as-deposited alloy had improved properties over annealed (O temper) 2219 plate, but less robust properties than T8 plate. It is expected that the mechanical properties of these deposits would be further enhanced with a T6 temper, provided that in future work the cracking problem would be solved by further optimization of the processing parameters for each alloy.

	YS (ksi)	UTS (ksi)	% el
2219, L As-deposited	17.8 ± 0.5	38.9 ± 2.2	25.6 ± 1.2
2219, L Direct Aged	17.8 ± 1.0	33.3 ± 1.1	22.0 ± 1.3
2139, L As-deposited	32.2 ± 1.9	51.7 ± 2.4	21.7 ± 0.5
2139, L Direct Aged	35.2 ± 6.3	47.4 ± 3.6	16.7 ± 6.8

	YS (ksi)	UTS (ksi)	% el
2219, ST As-deposited	15.9 ± 0.2	19.1 ± 1.3	1.0 ± 0.3
2219, ST Direct Aged	15.5 ± 0.4	18.4 ± 2.1	1.0 ± 0.6
2139, ST As-deposited	30.4 ± 8.3	41.1 ± 6.3	3.4 ± 1.6
2139, ST Direct Aged	23.1 ± 7.7	30.7 ± 13.2	3.0 ± 1.8

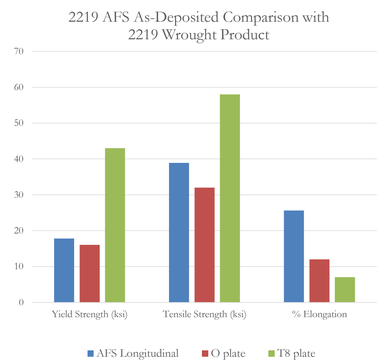

The ductility results indicated that necking occurred before failure in the L-tensile specimens for both alloys, although secondary cracking was observed, likely associated with the previously mentioned cracking. Across both alloys and heat treatment conditions, the ST-tensile samples exhibited elongations of just 0.4-5.0%, and inspection of the fracture surfaces revealed flat facets typical of interlayer separation. At higher magnifications, both L and ST samples exhibited small ductile dimples, however the 20-30% lower strength in the ST direction is clearly dominated by weak interfaces between deposit layers for these deposition parameters for both alloys.

Cracking Investigation

During sectioning of the specimens for imaging and mechanical testing sample extraction, it was discovered that the deposits were littered with cracks. These were particularly exaggerated in the samples that were solution heat treated and aged, likely due to thermal stresses during solutionizing and quenching. These cracks were investigated optically and with XCT (below), and are hypothesized to be from poor bonding between AFS layers.

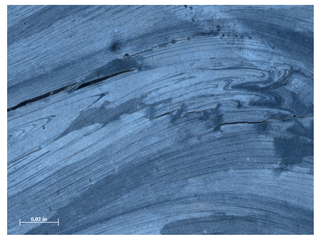

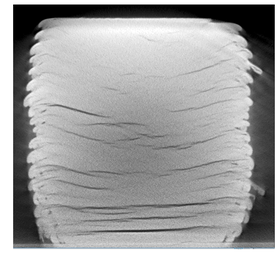

%SiC analysis of Al 6061 + SiC MMC Deposits

The final set of specimens explored in this work was AFS-deposited aluminum 6061+SiC MMC. The filler material for the additive friction stirring process was in the form of aluminum powder, with SiC content that could be varied based upon the desired percent reinforcement. Samples of nominal 0%, 5%, 10%, and 0-20 vol% SiC were delivered to NASA for evaluation of the MMC uniformity.

It was found that the 5 vol% SiC MMC deposit came the closest to meeting its specification for %SiC reinforcement. However, as the images below reveal, the percent reinforcement of SiC still varied dramatically over the height of the deposit, requiring further development of the processing methods to achieve uniform reinforcement throughout the build.

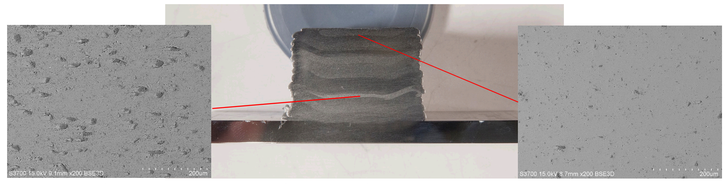

Al 6061 + 5 vol% SiC deposit with micrographs illustrating varying levels of SiC reinforcement across build height

To analyze for vol% SiC reinforcement, scanning electron microscope (SEM) micrographs of specific bands within the deposit were taken and energy dispersive spectroscopy (EDS) measurements were performed to highlight the Si in each image. The Si particles greater than 5μm were assumed to be SiC (rather than Si impurities), and the Si EDS map was fed into ImageJ, an image analysis program to determine the area percent of SiC in each micrograph.

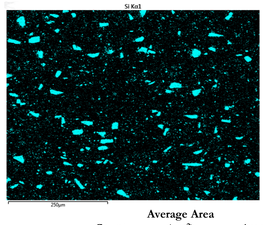

	Count	Average Area (μm²)	Area %
No size filter	2654	9.92	8.01
2μm dia. and up	897	25.84	7.05
5μm dia. and up	167	107.74	5.47
7μm dia. and up	102	159.31	4.94
10μm dia. and up	71	203.34	4.39

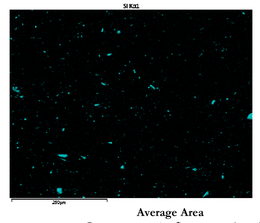

	Count	Average Area (μm²)	Area %
No size filter	476	7.25	1.13
2μm dia. and up	207	14.57	0.99
5μm dia. and up	28	59.90	0.55
7μm dia. and up	15	87.98	0.43
10μm dia. and up	5	154.17	0.25

Conclusions to date

The preliminary results from this work characterizing AFS deposits of Al 2219, 2139, and 6061+SiC look promising. While there were issues with cracks in the as-deposited samples that were accentuated during solutionizing, these may be addressed by optimizing processing parameters to promote better inter-layer bonding. Useful techniques for screening samples with XCT scanning and analyzing percent reinforcement of SiC were also developed for future use.